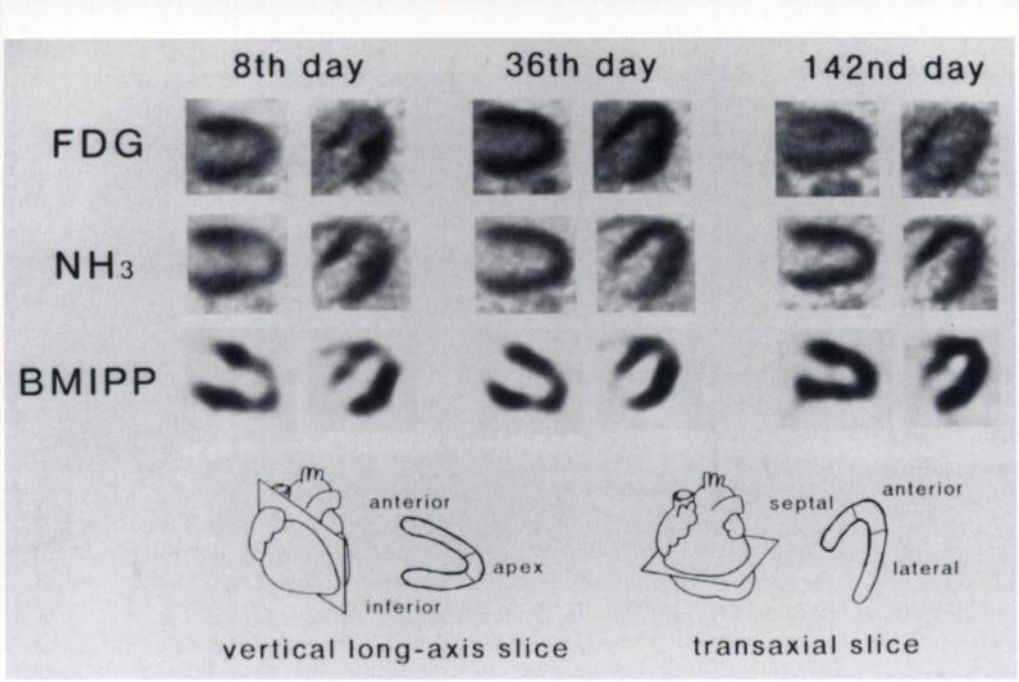

FIGURE 3. PET and BMIPP images (vertical long-axis and transaxial slices through the midleft ventricle), and the schema of myocardial segments of PET and BMIPP images. On the 8th day after onset, FDG uptake in the anterior and septal regions were relatively lower than that in the remote region. This relative reduction in FDG uptake was not observed on the 36th day. About 5 mo later, FDG uptake in the left ventricular myocardium significantly decreased. Nitrogen-13-ammonia uptake decreased in the anterior and septal regions on the 8th day, but this decreased uptake improved in the chronic phase. BMIPP uptake in the anterior and septal regions were relatively lower than that in the remote region on the 8th and 36th days, but improved at 5 mo after onset.

CONCLUSION

Metabolic abnormalities in stunned myocardium are sustained despite recovery from functional impairment; recovery from these abnormalities requires considerable time. The time course of the electrocardiographic recovery of deep negative T waves appeared to be related to the recovery of impaired energy metabolism in stunned myocardium in this patient.

REFERENCES

1. Braunwald E, Kloner RA. The stunned myocardium: prolonged, postischemic ventricular dysfunction. *Circulation* 1982;66:1146–1149.
2. Schwaiger M, Schelbert H, Ellison D, et al. Sustained regional abnormalities in cardiac metabolism after transient ischemia in the chronic dog model. *J Am Coll Cardiol* 1985;6:336–347.
3. Buxton D, Schelbert H. Measurement of regional glucose metabolic rates in reperfused myocardium. *Am J Physiol* 1991;261:H2058–H2068.
4. Tillisch J, Brunken R, Marshall R, et al. Reversibility of cardiac wall motion abnormalities predicted by positron tomography. *N Engl J Med* 1986;314:884–888.
5. Tamaki N, Yonekura Y, Yamashita K, et al. Positron emission tomography using fluorine-18 deoxyglucose in evaluation of coronary artery bypass grafting. *Am J Cardiol* 1989;64:860–865.
6. Tamaki N, Kawamoto M, Yonekura Y, et al. Regional metabolic abnormality in relation to perfusion and wall motion in patients with myocardial infarction: assessment with emission tomography using an iodinated branched fatty acid analog. *J Nucl Med* 1992;33:659–667.
7. Gelberg HJ, Brundage BH, Glantz S, Parmley WW. Quantitative left ventricular wall motion analysis: a comparison of area, chord and radial methods. *Circulation* 1979;59:991–1000.
8. Schwaiger M, Brunken R, Grover-Mckay M, et al. Regional myocardial metabolism in patient with acute myocardial infarction assessed by positron emission tomography. *J Am Coll Cardiol* 1986;8:800–808.
9. Matsunari I, Saga T, Taki J, et al. Improved myocardial fatty acid utilization after percutaneous transluminal coronary angioplasty. *J Nucl Med* 1995;36:1605–1607.
10. Tamaki N, Yonekura Y, Kawamoto M, et al. Simple quantification of regional myocardial uptake of fliorine-18-deoxyglucose in the fasting condition. *J Nucl Med* 1991;32:2152–2157.
11. ParodiP, Schelbelt HR, Schwaiger M, Hansen H, Selin C, Hoffman EJ. Cardiac emission computed tomography: underestimation of regional tracer concentrations due to wall motion abnormalities. *J Comput Assist Tomogr* 1984;8:1083–1092.

Acute Myocardial Infarction Followed by Technetium-99m-Sestamibi SPECT Imaging and Pathologic Correlation

David G. Hurrell, William D. Edwards, Michael K. O'Connor and Raymond J. Gibbons

Divisions of Cardiovascular Diseases and Internal Medicine, and Anatomic Pathology; and Section of Nuclear Medicine, Mayo Clinic, Mayo Foundation, Rochester, Minnesota

A 79-yr-old man received thrombolytic therapy for acute myocardial infarction after injection with ^{99m}Tc-sestamibi and died shortly thereafter. Postmortem in situ SPECT imaging of the heart was performed. The heart was then removed and sectioned into short-axis slices, which were placed directly on the SPECT camera face for imaging, and examined by routine gross and microscopic pathologic methods. Pathologic findings were consistent with a small acute inferoseptal myocardial infarction, as demonstrated on both SPECT imaging of the intact heart and imaging of the heart slices. This case report provides further evidence of the validity of SPECT sestamibi imaging for the determination of myocardium at risk during acute myocardial infarction.

Key Words: myocardial infarction; technetium-99m-sestamibi; thrombolytic therapy; SPECT

J Nucl Med 1997; 38:1837–1840

Received Dec. 12, 1996; accepted Mar. 10, 1997.

For correspondence or reprints contact: Raymond J. Gibbons, MD, Nuclear Cardiology Laboratory, Charlton 2, Mayo Clinic, Rochester, MN 55905.

The amount of myocardial salvage after acute infarction is a useful endpoint in the assessment of cardiovascular therapies (*1*). The assessment of myocardial salvage requires an accurate

determination of the myocardium at risk at the time of patient presentation and the final infarct size (myocardial salvage = myocardium at risk − infarct size). Using ^{99m}Tc-sestamibi SPECT imaging techniques, studies in animal models have validated the quantitative assessment of both myocardium at risk and infarct size (*2–3*).The measurement of infarct size in patients is closely associated with the amount of fibrosis in human hearts explanted at the time of cardiac transplantation (*4*). However, the myocardium at risk, expressed as a percentage of the left ventricular myocardium before the initiation of therapy, has not been validated in humans. We report a patient who received thrombolytic therapy for acute myocardial infarction shortly after injection with ^{99m}Tc-sestamibi and died, allowing a correlation of the myocardium at risk by both perfusion imaging and pathologic specimen.

CASE REPORT

A 79-yr-old man had a 5-yr history of infrequent bouts of exertional chest heaviness treated with sublingual nitroglycerin. Two months before hospital admission, he noted more frequent episodes of the same discomfort which occurred after walking two blocks. The symptoms were now more severe and required two sublingual nitroglycerin for complete relief.

On the morning of his hospital admission, he awoke at 6:30 am with severe chest discomfort radiating into both arms which was not relieved by five sublingual nitroglycerins. Two hours later, the pain persisted and he was taken to the hospital emergency room 2.5 hr following the onset of his chest pain. The physical examination was notable for a blood pressure of 110/60 mm Hg and an irregular pulse of 112 bpm. His jugular venous pressure was elevated to 12 cm of H_20. There was a 2/6 systolic ejection murmur at the left ventricular apex; no gallop was present. An electrocardiogram revealed atrial fibrillation and an acute inferior myocardial infarction with 2 mm of ST elevation in leads III and AVF, as well as 3 mm of ST depression in leads I, AVL, V2-V6. There were Q waves in leads V1 and V2. The creatinine kinase was 79 ng/ml.

The patient was diagnosed with an acute inferior myocardial infarction, as well as a possibly old anteroseptal myocardial infarction. He gave informed consent to participate in a research study of ^{99m}Tc-sestamibi in myocardial infarction. He was injected with 30 mCi ^{99m}Tc-sestamibi intravenously. His pain was relieved with four sublingual nitroglycerins. In addition, he received O_2 2 liters by nasal cannula, intravenous heparin (5000 U bolus followed by 1000 U/hr), metoprolol (5 mg intravenous bolus and 75 mg orally), a nitroglycerin drip (0.4 mg/kg intravenously) and lidocaine (75 mg bolus then 2 mg/min intravenous drip). Tissue plasminogen activator was administered (15 mg intravenous bolus, 50 mg over 30 min and 35 mg over the remaining 60 min) beginning 3.5 hr following the onset of his pain. The patient remained pain free and was admitted to the cardiac intensive care unit.

Three hours later, the patient was transferred to the nuclear cardiology laboratory for SPECT imaging. During imaging he became diaphoretic and bradycardic. Resuscitation efforts were initiated with epinephrine, dopamine and atropine. The patient was intubated and externally paced. Plans were being made for emergent cardiac catheterization when the patient developed electrical-mechanical dissociation. He died enroute to the catheterization laboratory 6 hr following his admission to the hospital.

The patient's family gave permission for a postmortem examination, including in situ imaging of the heart. The cadaver was then moved to the nuclear cardiology laboratory where SPECT imaging was performed 10 hr after isotope injection. Images were acquired using a rotating gamma camera with an all-purpose collimator. Thirty images were acquired for 40 sec each at every 6° throughout a 180° arc beginning 45° left anterior oblique (*5–6*). Processing and reconstruction were performed using standard backprojection algorithms and a Ramp-Hanning filter. Reconstruction was hampered by a minimal ventricular cavity, due to postmortem contraction (*7*). Circumferential count profiles were generated for five representative short-axis slices of the left ventricle extending from apex to base. The myocardium at risk was quantified using previously described methods and a threshold value of 60% of peak counts. The limit for detection of infarction by this technique has been shown to be 3% of the left ventricle (*5–6*).

There was a severe perfusion defect involving the inferoseptal wall at the base and midventricle which measured 5% of the left ventricle. While mild-to-moderate perfusion defects were apparent at the apical lateral wall and region of the anterolateral papillary muscle, they did not reach the threshold for quantitation. Representative tomographic images are displayed in Figure 1.

The cadaver was returned to the autopsy room. The heart was then removed and sectioned into short axis slides approximately 1 cm thick. The fresh heart slices were taken to the nuclear cardiology laboratory and placed directly on the SPECT camera surface for imaging. Count acquisition was performed over a 6-hr period. Representative tomographic images are displayed in Figure 1.

Pathologic Description

After completion of the imaging, the ventricular slices were fixed in formalin and examined by routine gross and microscopic methods (*8*). As described for tomographic imaging, the size of the left ventricle resembled that of end systole. On gross inspection, a small old transmural myocardial infarction was identified in the apical lateral wall of the left ventricle. A recent infarct, microscopically 10–16 days old, involved the anterolateral papillary muscle of the mitral valve.

More importantly, an area of acute infarction was identified along the inferoseptal wall of the left ventricular cavity at the midventricular and basal levels. It was primarily a subendocardial process in the inferior wall and a transmural process in the septum. In addition, there was subendocardial extension into the inferobasal wall of the right ventricle. Representative pathologic slices are displayed in Figure 1. Microscopically, the process appeared to be 12–24 hr old and was focally associated with interstitial hemorrhage, suggesting reperfusion. The pathology findings described for this acute event were consistent with the quantitative defect identified by nuclear imaging. Gross pathology inspection also revealed critical four vessel atherosclerosis, however, a site of plaque rupture or thrombus formation could not be identified.

DISCUSSION

After an acute infarction, the extent of myocardial necrosis is determined by the duration of coronary occlusion, collateral flow, and most importantly, the myocardium at risk (*9*). By the determination of the myocardium at risk, myocardial salvage and infarct size SPECT sestamibi imaging has proven to be a valuable measurement tool in the assessment of therapeutics for acute myocardial infarction.

SPECT sestamibi measurements of infarct size have significant associations with overall patient mortality ($p = 0.009$), and cardiac mortality ($p < 0.001$) after discharge (*11*). Infarct size using this quantitative technique has been validated against pathological fibrosis in both animal models and humans using

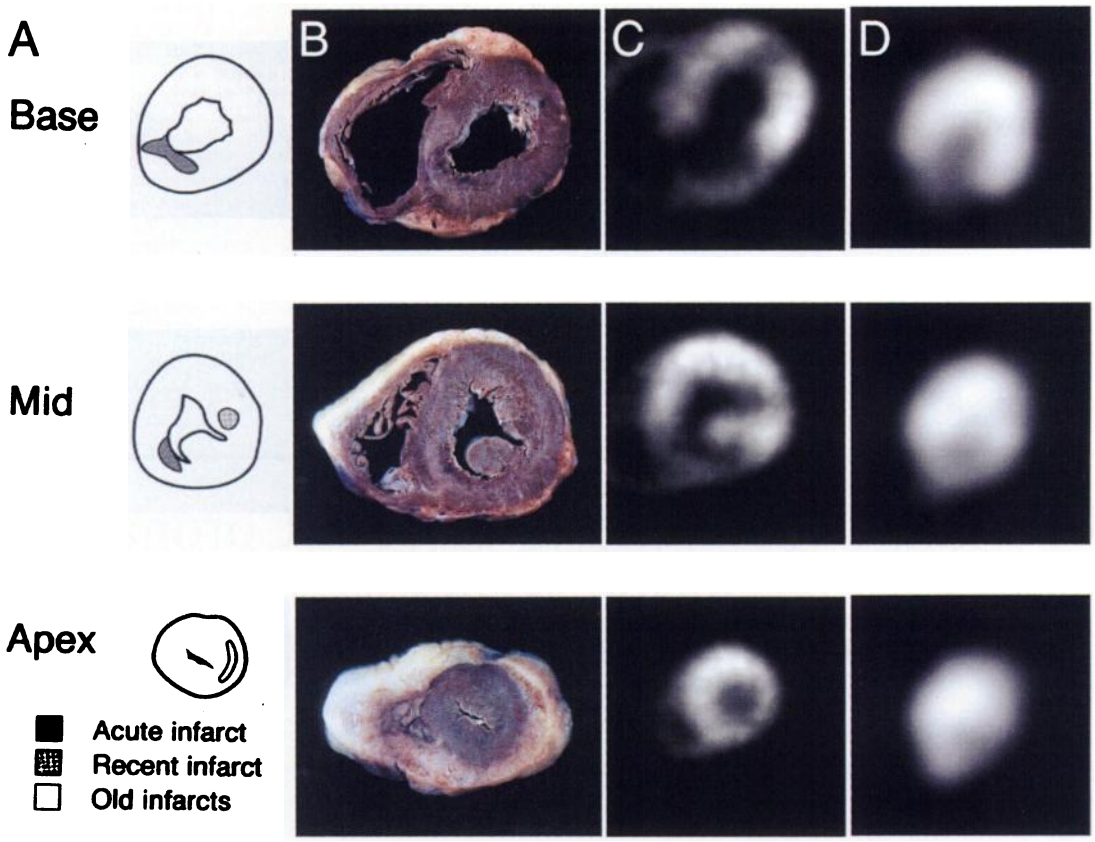

FIGURE 1. (A) Base, mid and apical slices of the left ventricle along with the myocardial infarctions and pathologic ages identified at autopsy. (B) Gross pathology specimens. Old infarction appears as white scar tissue while new infarction is most easily identified as hemorrhagic tissue. Note the total amount of myocardium involved by infarction is actually quite small. (C) After removal from the cadaver, the heart was sectioned into short-axis slides approximately 1 cm thick, and the slices were directly imaged on the camera surface. The image defects correlate with the identified infarctions found on the pathologic specimen. (D) SPECT images of the heart obtained postmortem. Total myocardium at risk was quantified at 5% of the left ventricle. Note that the heart remains at end systole after the patient's death which limits SPECT image quality.

explanted hearts (*2–4*). Although animal models have validated the measurement of myocardium at risk by this technique against angiographic measurements of risk area, similar measurements are not feasible in humans.

The myocardium at risk was first evaluated in the animal laboratory by Reimer et al. (*10*). In a model of circumflex occlusion, the myocardium at risk was highly variable and was the single most important determinant of infarct size. Subsequently, Feiring et al. (*12*) injected intracoronary radiolabeled macroaggregated albumin into the infarct-related artery before intracoronary thrombolysis in patients presenting with acute myocardial infarction. The myocardium at risk was variable between patients with the same infarct-related artery, similar to animal models. Despite the variability, there remained a significant association between myocardium at risk and early cardiac mortality ($p < 0.001$). In a subsequent study, Miller et al. (*11*) showed that myocardium at risk was also associated with 2-yr outcome ($p = 0.009$). Therefore, while this index has been defined in animal models and its clinical utility has been confirmed in patients, no reports have appeared which compare the measurement of the myocardium at risk in a human with pathologic correlation.

The patient described in this report presented with an acute myocardial infarction, was injected with ^{99m}Tc-sestamibi and died shortly after receiving thrombolytic therapy. Postmortem quantitative SPECT imaging was performed with the heart in situ to determine myocardium at risk. Pathological examination delineated the involved territory by acute ischemic changes. The SPECT imaging identified a clinically silent old apical lateral and anterolateral papillary muscle infarction which did not meet quantitative criteria, as well as a new inferoseptal infarction which measured 5% of the left ventricle. While no intracoronary thrombus was identified at autopsy, the patient had received thrombolytic therapy, and thrombus that was present at clinical presentation may have dissipated with therapy. This hypothesis was also supported by the pathology findings suggestive of successful reperfusion, despite the patient's death.

CONCLUSION

This case report provides further evidence of the validity of SPECT sestamibi imaging for the determination of myocardium at risk. Studies previously described and presently underway have begun to use the determination of myocardial salvage and infarct size for the evaluation of new therapeutic drugs and strategies. These techniques permit small pilot studies of new therapies without the enormous expense of mega-trials (*13*).

ACKNOWLEDGMENTS

This study was supported by a grant from DuPont Merck Pharmaceuticals Company.

REFERENCES

1. Gibbons RJ, Holmes DR, Reeder GS, Bailey KR, Hopfenspirger MR, Gersh BJ. Immediate angioplasty compared with the administration of a thrombolytic agent followed by conservative treatment for myocardial infarction. *N Engl J Med* 1993; 328:685–691.
2. Verani MS, Jeroudi MO, Mahmarian JJ, et al. Quantification of myocardial infarction during coronary occlusion and myocardial salvage after reperfusion using cardiac imaging with technetium-99m-hexakis-2-methoxy-isobutyl-isonitrile. *J Am Coll Cardiol* 1988;12:1573–1581.

3. Sinusas AJ, Trautman KA, Bergin JD, et al. Quantification of area at risk during coronary occlusion and degree of myocardial salvage after reperfusion with technetium-99m-methoxyisobutyl-isonitrile. *Circulation* 1990;82:1424–1437.
4. Medrano R, Weilbaacher D, Young JB, et al. Assessment of myocardial viability with technetium-99m sestamibi in patients undergoing cardiac transplantation: a scintigraphic-pathologic study [Abstract]. *Circulation* 1992;86(suppl I):I-108.
5. Gibbons RJ, Verani MS, Behrenbeck T, et al. Feasibility of tomographic ^{99m}Tc-hexakis-2 methoxy-2 methylpropyl-isonitrile imaging for the assessment of myocardial area at risk and the effect of treatment in acute myocardial infarction. *Circulation* 1989;80:1277–1286.
6. O'Connor MK, Hammell TC, Gibbons RJ. In vitro validation of a simple tomographic technique for estimation of percent myocardium at risk following administration of Tc99m isonitrile. *Eur J Nucl Med* 1990;17:69–76.
7. Maron BJ, Henry WL, Roberts WC, et al. Comparison of echocardiographic and necropsy measurements of ventricular wall thicknesses in patients with and without disproportionate septal thickening. *Circulation* 1977;55:341–346.
8. Edwards WD. Pathology of myocardial infarction and reperfusion. In: Gersh BJ, Rahimtoola SH, eds. *Acute myocardial infarction*. New York: Elsevior; 1991:14–48.
9. Lowe JE, Reimer KA, Jennings RB. Experimental infarct size as a function of the amount of myocardium at risk. *Am J Pathol* 1978;90:373–376.
10. Reimer KA, Jennings RB, Cobb RF, et al. Animal models for protecting ischemic myocardium: results of the NHLBI Cooperative Study. Comparison of unconscious and conscious dog models. *Circ Res* 1985;56:651–665.
11. Miller TD, Christian TF, Hopfenspirger MR, Hodge DO, Gersh BJ, Gibbons RJ. Infarct size after acute myocardial infarction measured by quantitative tomographic ^{99m}Tc sestamibi imaging predicts subsequent mortality. *Circulation* 1995;92:334–341.
12. Feiring AJ, Johnson MR, Kioschos JM, Kirchner PT, Marcus ML, White CW. The importance of the determination of the myocardial area at risk in the evaluation of the outcome of acute myocardial infarction in patients. *Circulation* 1987;75:980–987.
13. Gibbons RJ, Christian TF, Hopfenspirger M, Hodge DO, Bailey KR. Myocardium at risk and infarct size after thrombolytic therapy for acute myocardial infarction: implications for the design of randomized trials of acute intervention. *J Am Coll Cardiol* 1994;24:616–623.

Technetium-99m MIBI to Assess Coronary Collateral Flow During Acute Myocardial Infarction in Two Closed-Chest Animal Models

Timothy F. Christian, Michael K. O'Connor, Robert S. Schwartz, Raymond J. Gibbons and Erik L. Ritman
Division of Cardiovascular Diseases and Internal Medicine and Departments of Nuclear Medicine and Physiology, Mayo Clinic and Mayo Foundation, Rochester, Minnesota

Collateral flow is an independent determinant of infarct size in both animal and clinical studies of myocardial infarction. The purpose of this study was to quantitatively evaluate, in a closed-chest animal model, a noninvasive method of measuring coronary collateral flow over a wide spectrum of collateral flow rates from a tracer that can be injected during occlusion but measured after reperfusion. **Methods:** Fourteen animals underwent 40 min of coronary occlusion using a closed-chest technique. Two closed-chest models representing different rates of collateral flow were used: canine and porcine. Coronary blood flow was measured by radiolabeled microspheres. Collateral blood within the risk zone was estimated from the severity of ^{99m}Tc-sestamibi tomographic perfusion defect. **Results:** Collateral blood flow was significantly higher in the canine model than it was in the porcine model. There was close agreement ($r = 0.90$) between absolute collateral flow by microspheres and the severity of the tomographic perfusion defect. **Conclusion:** These results suggest that an accurate noninvasive estimate of collateral blood flow can be provided by an intravenous injection of ^{99m}Tc-sestamibi.

Key Words: collateral circulation; radionuclide imaging; coronary blood flow

J Nucl Med 1997; 38:1840–1846

Collateral flow to jeopardized myocardium is an important determinant of outcome during acute myocardial infarction. Animal studies of reperfusion have established the magnitude of collateral flow as one of the four independent determinants of infarct size (in addition to the extent of the risk area, metabolic demand and duration of occlusion) (*1,2*) and as the primary factor in extending the window of time for which late coronary reperfusion can be of benefit (*2*). The importance of collateral flow as a determinant of infarct size has been confirmed in clinical studies (*3–5*). However, assessment of collateral flow in patients during acute myocardial infarction is still a problem. Angiographic assessment of collaterals is strongly associated with subsequent outcome during myocardial infarction but is not always available or feasible before thrombolytic therapy (*3–6*). Invasive contrast echocardiography has been used in the weeks after infarction to assess collateral flow but has not been used clinically with an intravenous injection during acute myocardial infarction (*7*).

In a previous clinical study, we described the use of the severity of the perfusion defect by tomographic perfusion imaging after the intravenous injection with ^{99m}Tc-sestamibi to assess collateral flow during the acute stages of myocardial infarction (*4*). This measurement was strongly associated with the presence of angiographic collaterals before reperfusion therapy and was a significant determinant of final infarct size, which was independent of myocardium at risk and time to reperfusion. The purpose of this study was to validate a noninvasive tomographic imaging method for the assessment of collateral flow, which can be initiated during coronary artery occlusion but acquired after reperfusion by comparing its performance to true myocardial blood flow during occlusion, determined by radiolabeled microspheres in closed-chest animal models. This replicates the clinical situation for which this technique has been used (*4*). To test this measure over a range of collateral flows, two models were used: a canine model, in which native collateral flow is expected to be high; and a porcine model, in which native collateral flow is expected to be low.

MATERIALS AND METHODS

Experimental Preparation Methods

Two models were used in this study. Seven mongrel dogs (weight 27 ± 2 kg; range 24 kg–29 kg) and eight pigs (weight 38 ± 5 kg; range 32 kg–45 kg) underwent general anesthesia with intravenous pentobarbitol, fentanyl and droperidol (dogs) or ketamine and fentanyl (pigs), for the canine and porcine models,

Received Aug. 13, 1996; revision accepted Feb. 24, 1997.
For correspondence or reprints contact: Timothy F. Christian, MD, Mayo Clinic, 200 First Street Southwest, East 16B, Rochester, MN 55905.